The Journal of Immunology

Dermal Enhancement: Bacterial Products on Intact Skin Induce and Augment Organ-Specific Autoimmune Disease

D. Sean Riminton, Rama Kandasamy, Danijela Dravec, Antony Basten and Alan G. Baxter

J Immunol 2004; 172:302-309; ;
doi: 10.4049/jimmunol.172.1.302
http://www.jimmunol.org/content/172/1/302

The Journal of Immunology is published twice each month by
The American Association of Immunologists, Inc.,
1451 Rockville Pike, Suite 650, Rockville, MD 20852

Print ISSN: 0022-1767 Online ISSN: 1550-6606.

Dermal Enhancement: Bacterial Products on Intact Skin Induce and Augment Organ-Specific Autoimmune Disease[1]

D. Sean Riminton,[†] Rama Kandasamy,[†] Danijela Dravec,[†] Antony Basten,[†] and Alan G. Baxter[2]*

The skin is both an essential barrier for host defense and an important organ of immunity. In this study, we show that the application of cholera toxin to intact mouse skin induces and enhances autoimmune diseases affecting organs at distant anatomic sites, whereas its administration by the mucosal route has been reported to have the opposite effect. First, the CNS autoantigen myelin oligodendrocyte glycoprotein 35–55, when applied repeatedly with cholera toxin to the intact skin of healthy C57BL/6 mice, induced relapsing paralysis with demyelinating immunopathologic features similar to multiple sclerosis. Second, the application of cholera toxin in the absence of autoantigen exacerbated the severity of conventional experimental autoimmune encephalomyelitis induced by myelin oligodendrocyte glycoprotein in CFA. Third, the application of cholera toxin to the intact skin of NOD/Lt mice, with or without insulin B peptide 9–23, exacerbated insulitis and T lymphocyte-derived IFN-γ and IL-4 production in the islets of Langerhans, resulting in an increased incidence and rate of onset of autoimmune diabetes. The data presented in this study highlight the different outcomes of adjuvant administration by different routes. Because dermal application of cholera toxin, and other bacterial products with similar adjuvant activities, is being developed as a clinical vaccination strategy, these data raise the possibility that it could precipitate autoimmune disease in genetically susceptible humans. ***The Journal of Immunology*****, 2004, 172: 302–309.**

Application of bacterial ADP ribosylating exotoxins, such as cholera toxin (CT),[3] to the intact skin in an aqueous mixture with a vaccine Ag induces systemic immune responses to both toxin and Ag, whereas application of the vaccine Ag alone has no effect (1, 2). This phenomenon provides new insights into the cutaneous immune system, emphasizing the existence of a dynamic interaction with the external environment that has significant effects on systemic immunity. Dermal immunization by this and comparable techniques has now been demonstrated in a variety of mammalian species, including humans, and forms the basis for novel vaccination strategies currently under development for human infectious disease prophylaxis (3–5). This manuscript describes the effects of a bacterial toxin applied to intact skin, with or without self-Ag, on the clinical and immunopathological processes of autoimmunity.

Materials and Methods

Mice

Female C57BL/6 mice were supplied by the Animal Resources Centre (Perth, Australia) and female NOD/Lt mice by The Jackson Laboratory (Bar Harbor, ME). All mice were maintained under clean conventional conditions in the Animal Facility of the Centenary Institute of Cancer Medicine and Cell Biology (Sydney, Australia) in accordance with institutional guidelines and approved by the Animal Care and Ethics Committee of the University of Sydney (Sydney, Australia). Sentinel mice were tested by serology at 4-mo intervals for significant mouse pathogens without any evidence of infection being detected.

CFA/myelin oligodendrocyte glycoprotein (MOG)$_{35–55}$ induced experimental autoimmune encephalomyelitis (EAE)

EAE was actively induced in pertussis toxin (PT; two doses of 200 ng i.v.) pretreated C57BL/6 mice with an emulsion of 50 μg of MOG$_{35–55}$ in CFA as previously described (6).

Dermal immunization

This procedure was performed as previously described (2). Briefly, mice were shaved on the dorsum and rested for at least 24 h. While under anesthesia (ketamine 4 mg + xylazine 0.2 mg i.p.), the shaved area was swabbed with 70% isopropanol before 150 μl of solution were applied without further manipulation to the skin surface for 1 h. 1) EAE: C57BL/6 mice received 50 or 100 μg of MOG$_{35–55}$ (35-MEVGWYRSPFSRVVH-LYRNGK-55, Ref. 7) peptide and/or 100 or 200 μg of CT (List Biological Laboratories, Campbell, CA). The immunized area was washed twice with water after 1 h. PT (200 ng) was injected i.v. on days 0 and 2 of each immunization. 2) Diabetes: NOD/Lt mice were treated with PBS alone, CT (100 μg) alone or insulin (INS) B$_{9–23}$ (9-SHLVEALYLVCGERG-23, Ref. 8; Mimotopes, Clayton, Australia) (100 μg), together with CT (100 μg). Each solution was administered to the swabbed area for 1 h as above.

All animals underwent four rounds of immunization separated by 21 days between each round unless otherwise stated.

Monitoring of diabetes in, and pancreatic histology of, NOD/Lt mice

Blood glucose estimations were performed as previously described (9). Mice with blood glucose readings of $\geq$11.1 mM on two consecutive occasions were classified as diabetic. Proportional hazards (Cox) regression modeling was applied to diabetes Kaplan Meier curves, with the hazard ratio representing the relative risk over time of achieving the diabetes end-point when compared with the control group, which was arbitrarily assigned a hazard value of 1.0. For histological assessment of islet infiltration, pancreata were fixed in 10% formalin in saline and paraffin-embedded. Three serial 5-μm sections were cut at each of three levels 100 μm apart and stained with H&E. Each islet was examined at 100$\times$ and given a score from 0 to 4 in which 0

*Comparative Genomics Centre, James Cook University, Townsville, Queensland, Australia; and [†]Centenary Institute of Cancer Medicine and Cell Biology, Newtown, New South Wales, Australia

Received for publication May 8, 2003. Accepted for publication October 27, 2003.

The costs of publication of this article were defrayed in part by the payment of page charges. This article must therefore be hereby marked *advertisement* in accordance with 18 U.S.C. Section 1734 solely to indicate this fact.

[1] This work was supported by a Development Grant from the National Health and Medical Research Council of Australia.

[2] Address correspondence and reprint requests to Dr. Alan G. Baxter, Comparative Genomics Centre, James Cook University, Molecular Sciences Building 21, Townsville, Queensland 4811, Australia. E-mail address: Alan.Baxter@jcu.edu.au

[3] Abbreviations used in this paper: CT, cholera toxin; MOG, myelin oligodendrocyte glycoprotein; EAE, experimental autoimmune encephalomyelitis; INS, insulin; PT, pertussis toxin; TLR, Toll-like receptor; LT, heat labile enterotoxin.

0022-1767/04/$02.00

represented a noninfiltrated islet and 4 represented complete infiltration or a "burnt-out" islet. The insulitis score for each mouse was calculated by expressing the total of the scores as a percentage of the sum of the maximum possible scores (9).

Neuropathology

Animals were monitored daily, and neurological deficits were quantified on a scale from 0 to 6 (6). Animals with multifocal deficits were scored according to the following scale: 0, normal; 1, hunched back; 2, abnormal gait; 3, severely hunchbacked, difficulty to right from supine; 4, hind limb paralysis, loss of ability to right from supine position, flaccid tail; 5, forelimb weakness, moribund; 6, death. CNS tissue, obtained from animals sacrificed 30 days following onset of motor deficits, was processed following perfusion as described (6). Where statistical comparisons between groups were made, scores for individual mice at each time point were normalized by subtraction of the mean score for the control group at that time point. All scores from each group were then compared using the Mann-Whitney test.

Assessment of cytokine production

EAE model. CFA/$MOG_{35–55}$ immunized mice and a group of mice having previously undergone four CT/$MOG_{35–55}$ treatment rounds, were boosted with CT/$MOG_{35–55}$ peptide as above. Neither group received PT injections for this immunization. Splenocytes (3×10^5 viable cells/well) were harvested 5 days later and stimulated in vitro with $MOG_{35–55}$ peptide (40 μg/ml), CT (20 μg/ml), or cultured without stimulation as a negative control. To reduce CT toxicity, monosialoganglioside-GM1 (14 μg/ml; Sigma-Aldrich, St. Louis, MO) was added to CT before addition to cultures. Supernatants were collected after 24 h. Supernatants were analyzed for the presence of IFN-γ using a Quantakine Immunoassay kit (R&D Systems, Minneapolis, MN) and IL-4 by ELISA as previously described (9).

NOD/Lt diabetes model. Pancreatic leukocytes were incubated with plate-bound KT3 (anti-CD3) (10) for 6 h at 37°C, 5% CO_2, and 99% humidity. IFN-γ secretion was assayed using a Cytokine ELISPOT set (BD PharMingen, San Diego, CA). IL-4 secretion was assayed by the same protocol as for IFN-γ except for the use of 11B11 (anti-IL-4; BD PharMingen) and BVD6-biotin (anti-IL-4; BD PharMingen) as primary and secondary Abs, respectively.

Assessment of Ab production

Sera were screened for autoantigenic peptide-specific ($MOG_{35–55}$ and INS $B_{9–23}$) and CT-specific IgG responses by ELISA. Anti-autoantigenic peptide-specific IgG plates were coated with avidin followed by biotinylated peptide (Mimotopes, Clayton, Australia) while anti-CT-specific IgG plates were coated with CT. Ab was detected with HRP-conjugated goat anti-mouse IgG (H+L; Pierce, Rockford, IL). Product was revealed using 2,2′-azinobis(3-ethylbenzthiazoline-6-sulfonic acid) (Sigma-Aldrich).

Isolation and analysis of pancreatic infiltrating leukocytes

Single cell suspensions of pancreata were washed twice ($300 \times g$ for 10 min at 4°C) and leukocytes extracted on a 37% Percoll gradient (Amersham Pharmacia Biotech, Uppsala, Sweden), washed in PBS, and resuspended in T cell medium (RPMI 1640 medium; Invitrogen, New York, NY; 1 mM Na-pyruvate, mercaptoethanol and FCS). Total leukocyte numbers were determined using a Sysmex KX-21 automated hematology analyzer (TOA Medical Electronics, Kobe, Japan). Pancreatic leukocytes were surface-stained in 96-well plates with anti-CD4-FITC (clone L3T4; BD PharMingen), anti-CD8a-PE (clone Ly-2; BD PharMingen), and anti-CD45 leukocyte common Ag (LCA)-biotin-PerCP (clone I3/2.3; Southern Biotechnology Associates, Birmingham, AL). Data for all samples were acquired on a FACSCalibur flow cytometer (BD Biosciences, Mountain View, CA) using CellQuest software (BD Immunocytometry Systems, San Jose, CA).

Splenic T cell proliferation

Single cell suspensions of splenocytes from 16-wk-old female NOD/Lt mice were washed twice ($300 \times g$ for 7 min at 4°C). Pellets were then resuspended in 4 ml of RBC lysis buffer (Sigma-Aldrich) for 10 min and washed twice before being resuspended in 1 ml of T cell medium. The pellet derived from APC donor NOD/Lt mouse spleens was resuspended in PBS and irradiated (2000 rad by cesium source, Gammacell 40 Exactor; Nordian International, Ottawa, Ontario, Canada). T cell-enriched splenocytes were prepared by two passages through nylon wool columns. Scrubbed nylon fiber (Fenwal Laboratories, Deerfield, IL) was soaked overnight in 0.2 M HCl, then washed thoroughly in distilled water and dried. Nylon wool columns were prepared by packing the nylon wool into polypropylene syringes (Terumo, Melbourne, Australia) at 0.1 g/ml. On the day of use, the nylon wool columns were prewashed with T cell medium. Splenocytes at 10^8 cells/ml in T cell medium were run onto the column. The columns were incubated at 37°C for 60 min. Nonadherent cells were washed and applied to another column of nylon wool, repeating the above procedure. Irradiated APC were added (2.5×10^5 viable cells/well) together with T cell-enriched splenocytes (1×10^5 viable cells/well) and stimulated in vitro with either INS $B_{9–23}$ (40 μg/ml), CT (20 μg/ml) with GM1 (14 μg/ml, to reduce in vitro CT toxicity), or cultured without stimulation as a negative control. T cell proliferative responses were quantified at 96 h after a 14-h pulse with [^{3}H]thymidine.

Results

Dermal application of CT with $MOG_{35–55}$ peptide induced EAE

The effects of dermal application of CT with the immunodominant $MOG_{35–55}$ peptide were examined in female C57BL/6 mice. Each mouse was treated on four to five occasions, 21 days apart, with either 100 μg of CT/50 μg of MOG, 200 μg of CT/50 μg of MOG, 100 μg of CT/100 μg of MOG or 200 μg of CT/100 μg of MOG (see Table I for treatment details). As a positive control, EAE was induced by conventional s.c. immunization with 50 μg of $MOG_{35–55}$ peptide emulsified in CFA (11) ($n = 33$, Table I). PT, which is necessary for the reproducible induction of active EAE (11), was administered i.v. (200 ng) to all animals on the day of each treatment and 2 days subsequently.

Table I. *Comparison between CT/$MOG_{35–55}$- and CFA/$MOG_{35–55}$-induced EAE*

	Treatment				Number Affected Following Tx[a]						Affected	Range in Time of Onset	Total Relapses
Group	MOG (mg)	CFA	CT (mg)	PT (ng)	*n*	Tx 1	Tx 2	Tx 3	Tx 4	Tx 5	(%)	(days)	(%)
CFA	50	+	−	200 ×2	33	29	NA	NA	NA	NA	29 (88)	12–14	−
CT Group A	50	−	100	200 ×2	6	−	−	−	5	NA	5 (83)	68–73	1
CT Group B	50	−	200	200 ×2	4	−	−	−	3	NA	3 (75)	76–87	1
CT Group C	100	−	100	200 ×2	5	−	−	1	4	NA	5 (100)	52–81	−
CT Group D	100	−	200	200 ×2	19	3	3	2	5	1	14 (74)	18–97	6
CT Summary	50− 100	−	100− 200	200 ×2	34	3	3	3	12	6	27 (79)	18–97	8 (40[b])

[a] NA = not applicable. Tx = treatment number with treatments on days 0, 21, 42, 63, and 84. Only mice treated with CT in group D received the fifth round of treatment.
[b] Percentage of CT recipients observed for at least 100 days that developed relapses following complete recovery from initial clinical deficits ($n = 8$ of 20).

As expected, mice immunized with CFA/$MOG_{35–55}$ developed transient EAE on or shortly after day 12 (Fig. 1*a*). Surprisingly, clinical neurological deficits characteristic of EAE were manifest in 27 of 34 (79%) of CT/$MOG_{35–55}$ recipients (Table I, Figs. 1, *b–e*, and 2*a*). The onset of EAE induced by CT/$MOG_{35–55}$ ranged from days 18 to 97 after initial treatment (median: day 71, Table I). Once initiated, EAE induced by CT/$MOG_{35–55}$ progressed rapidly to reach a peak of disease severity that was usually followed by gradual recovery. Two clinical syndromes were observed in mice with EAE induced by CT/$MOG_{35–55}$: ascending symmetrical motor deficits (4 of 27; Fig. 1*e*, mice 13 and 14), and more commonly, asymmetrical multifocal motor deficits (21 of 27; Fig. 1, mice 1–12 and 15). In contrast to the monophasic course of EAE induced by CFA/$MOG_{35–55}$, relapsing disease was observed in 8 of 20 (40%) mice treated with CT/$MOG_{35–55}$ and monitored for at least 100 days. In five such cases, the relapses were temporally associated with dermal application of CT (Fig. 1, mice 11, 14, and 15). The finding of relapsing disease is interesting because it is a characteristic feature of multiple sclerosis (Fig. 1*a*, Table I).

Neuropathology of CT/$MOG_{35–55}$-treated mice

Neuropathological findings in mice treated with CT/$MOG_{35–55}$ (Fig. 2*b*) were comparable to those found in EAE induced by CFA/$MOG_{35–55}$ (6). Specifically, the white matter was markedly disrupted by submeningeal and perivascular inflammatory cell infiltrates, identified by immunoperoxidase staining as comprising mainly macrophages and a smaller population of $CD4^+$ T lymphocytes (data not shown). Primary demyelination, in which myelin is lost from otherwise viable axons, was observed in subpial inflammatory areas including both motor and sensory neurons (Fig. 2*b*). Myelinated fibers in areas deep to inflammatory lesions, and in the peripheral nervous system and gray matter, where MOG is not expressed, were relatively preserved.

Immune responses following CT/$MOG_{35–55}$ peptide treatment

IgG anti-CT responses were consistent with exposure to CT (Fig. 2*c*), whereas Ab responses to $MOG_{35–55}$ peptide (Fig. 2*d*) were undetectable in mice treated with CT/$MOG_{35–55}$, even in animals

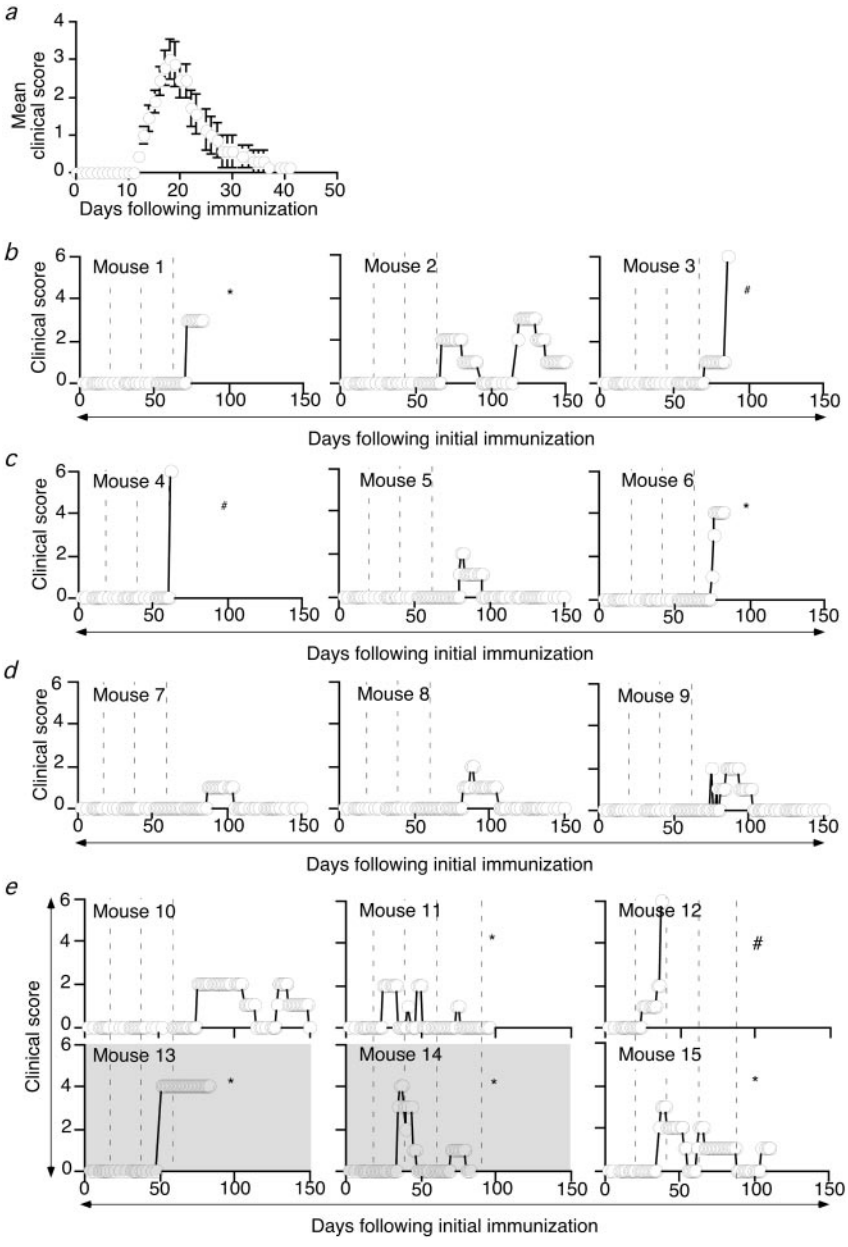

FIGURE 1. Natural history of EAE induced by CFA/$MOG_{35–55}$- and CT/$MOG_{35–55}$. *a*, Ascending and symmetrical neurological deficits developed following s.c. immunization of C57BL/6 mice with CFA/$MOG_{35–55}$ ($n = 9$; mean ± SE). *b-e*, EAE induced by CT in representative C57BL/6 mice (15 of 34) following treatment with CT. Details of results for all 34 mice are presented in Table I. Mice received treatment with 100 μg/50 μg of $MOG_{35–55}$ (*b*, 5 of 6 affected), 100 μg of CT/100 μg of $MOG_{35–55}$ (*c*, 5 of 5 affected), 200 μg of CT/50 μg of $MOG_{35–55}$ (*d*, 3 of 4 affected), and 200 μg of CT/100 μg of $MOG_{35–55}$ (*e*, 14 of 19 affected) on days 0, 21, 42, 63, and 84 (vertical dashed lines) following immunization. Mice 3, 4, and 12 were found dead (#) and mice 1, 6, 11, and 13–15 were harvested for further studies (∗).

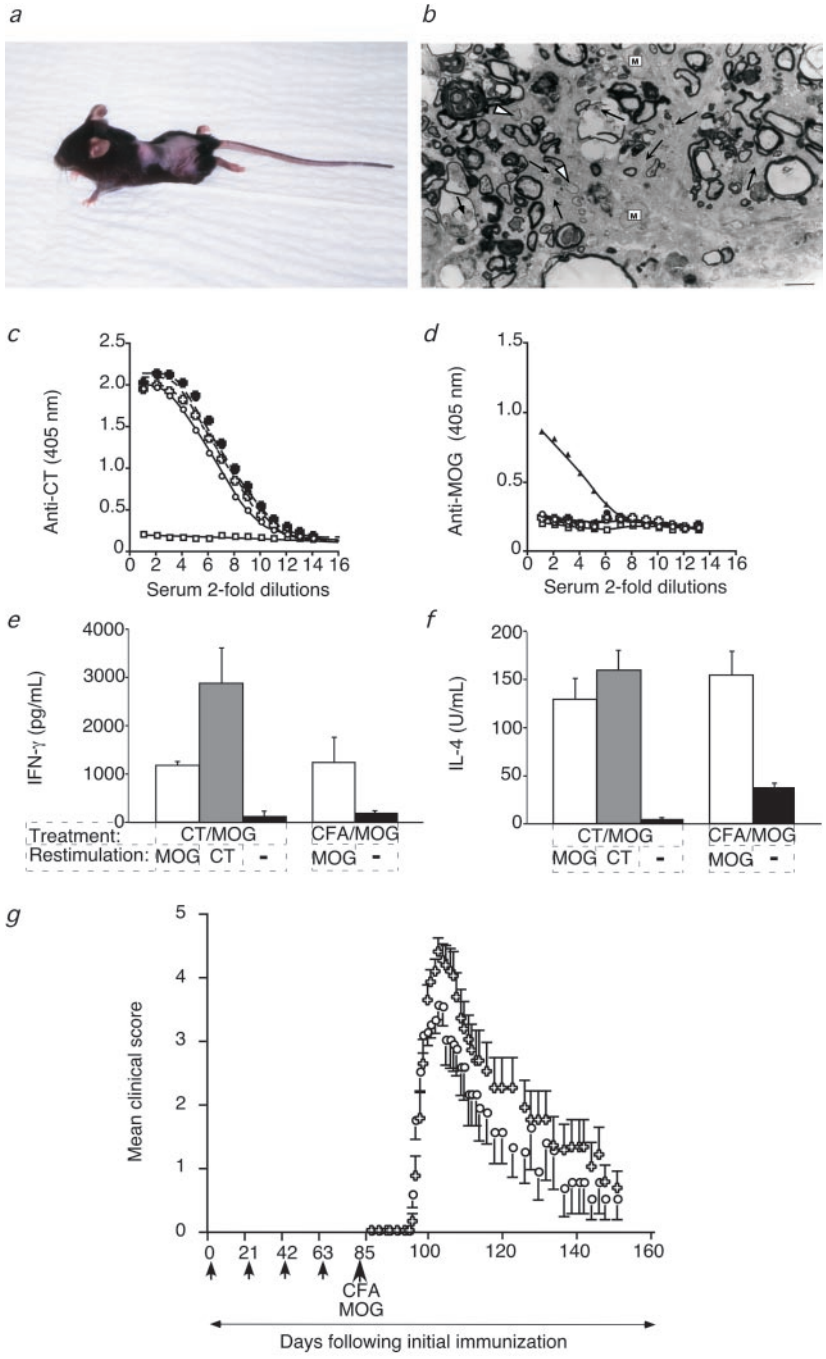

FIGURE 2. Clinical and immunopathological features of EAE induced by CT/$MOG_{35–55}$. *a*, Total hind-body paralysis in a recipient of CT/$MOG_{35–55}$ treatment. *b*, CT/$MOG_{35–55}$ induces demyelinating inflammatory changes in the CNS. Transverse tissue section of paraffin-embedded EAE-affected spinal cord (induced by CT/$MOG_{35–55}$ treatment) at day 40 following onset of disease. This section shows an area of inflammatory demyelination. Naked axons devoid of myelin are highlighted by arrows and thinly myelinated fibers by arrow heads. Lipid from myelin breakdown is evident within the phagocyte cells (M)-"glitter" cells. Irregular myelin profiles are plentiful representing active demyelination. Bar = 10 μm. *c* and *d*, Serum IgG anti-CT (*c*) and anti-$MOG_{35–55}$ peptide (*d*) responses following four rounds of 100 μg of CT/50 μg of $MOG_{35–55}$ (n = 5, ○), 100 μg of CT/100 μg of $MOG_{35–55}$ (n = 4, ✣), 200 μg of CT/50 μg of $MOG_{35–55}$ (n = 3, ●), or 200 μg of CT/100 μg of $MOG_{35–55}$ (n = 19, ✚). Normal mouse serum (n = 10, □) and anti-peptide Ab response from CFA/$MOG_{35–55}$ immunized mice (n = 9, ▲) are shown for comparison. *e* and *f*, IFN-γ (*e*) and IL-4 (*f*) cytokine production by spleen cells harvested at day 5 following immunization with either with CT/$MOG_{35–55}$ five times or CFA/$MOG_{35–55}$ once and restimulated in vitro with CT (in the presence of monosialoganglioside-GM1 to inhibit in vitro CT toxicity) or $MOG_{35–55}$ peptide. Results represent three similar experiments (mean ± SEM). *g*, Dermal application of CT before CFA/$MOG_{35–55}$ immunization enhances the severity of EAE (mean ± SE). Mice received either sham treatment (n = 16, ○), 100 μg of CT alone (n = 13, ✣) or 100 μg of CT/100 μg of $MOG_{35–55}$ (n = 18, data not shown) immunization (small arrows) followed by CFA/$MOG_{35–55}$ and PT (large arrow). The data for 100 μg of CT/100 μg of $MOG_{35–55}$ overlaid the 100 μg of CT alone data.

that had developed clinical manifestations of EAE. In contrast, splenocyte responses following restimulation in vitro with CT (in the presence of monosialoganglioside-GM1 to inhibit in vitro CT toxicity) or $MOG_{35–55}$ peptide were both characterized by IFN-γ, and to a lesser extent IL-4, production (Fig. 2, *e* and *f*). Moreover, the levels of IFN-γ and IL-4 secreted in response to $MOG_{35–55}$ peptide were comparable to those produced by splenocytes from $MOG_{35–55}$/CFA recipients (Fig. 2, *e* and *f*).

Dermal CT alone enhanced the severity of CFA/$MOG_{35–55}$-induced EAE

In the above experiments, CT induced EAE through the skin in an autoantigen-dependent manner. To examine the effect of dermal administration of CT alone on progression of EAE, mice were pretreated with four rounds of dermal application with saline, CT alone, or CT/$MOG_{35–55}$, in the absence of PT, before conventional induction of disease with PT and $MOG_{35–55}$/CFA. When CFA-induced disease developed (Fig. 2*g*), it was of greater severity and duration in mice preconditioned with either CT or CT/$MOG_{35–55}$; that is, dermal application of CT alone, without coadministration of autoantigen, enhanced autoimmune disease induced by other means ($p < 0.001$, Mann-Whitney test).

CT with or without INS $B_{9–23}$ peptide exacerbated autoimmune diabetes in NOD/Lt mice

The capacity of dermal administration of CT to enhance the severity of EAE in C57BL/6 mice raised the possibility that CT could modulate ongoing autoimmune responses. Therefore, we examined the effects of CT in a model of spontaneous autoimmune pathology, namely: autoimmune diabetes in NOD/Lt mice. Three

groups ($n = 30$) of female NOD/Lt mice received four dermal applications of the following treatments: group 1, sham treatment with PBS only; group 2, 100 μg of CT alone; and group 3, 100 μg of CT plus 100 μg of the immunodominant INS B_{9-23} (8). The onset of diabetes was accelerated in NOD/Lt mice treated with either CT alone or CT together with INS B_{9-23} peptide, compared with sham-treated controls ($p < 0.005$, log rank test, Fig. 3*a*). The incidence of diabetes at 30 wk of age was also significantly greater in both CT and CT/INS B_{9-23}-treated mice (54% group 1 vs 83% for groups 2 and 3 taken together, $p < 0.01$, Contingency Table Analysis, Fig. 3*a*). CT and the CT/INS B_{9-23}-treated mice were more likely to develop diabetes than controls (Hazard ratios 2.2 and 2.8, respectively). Although neither the time to onset of disease nor the final incidence of disease at 30 wk was significantly different between groups 2 and 3, there was a trend toward an earlier onset of diabetes in recipients of CT/INS B_{9-23} compared with those exposed to CT alone (Fig. 3*a*).

Insulitis in CT- and CT/INS B_{9-23}- treated NOD/Lt mice

The effect of dermal exposure to CT on the extent of islet inflammation (insulitis) was examined histologically within the pancreata

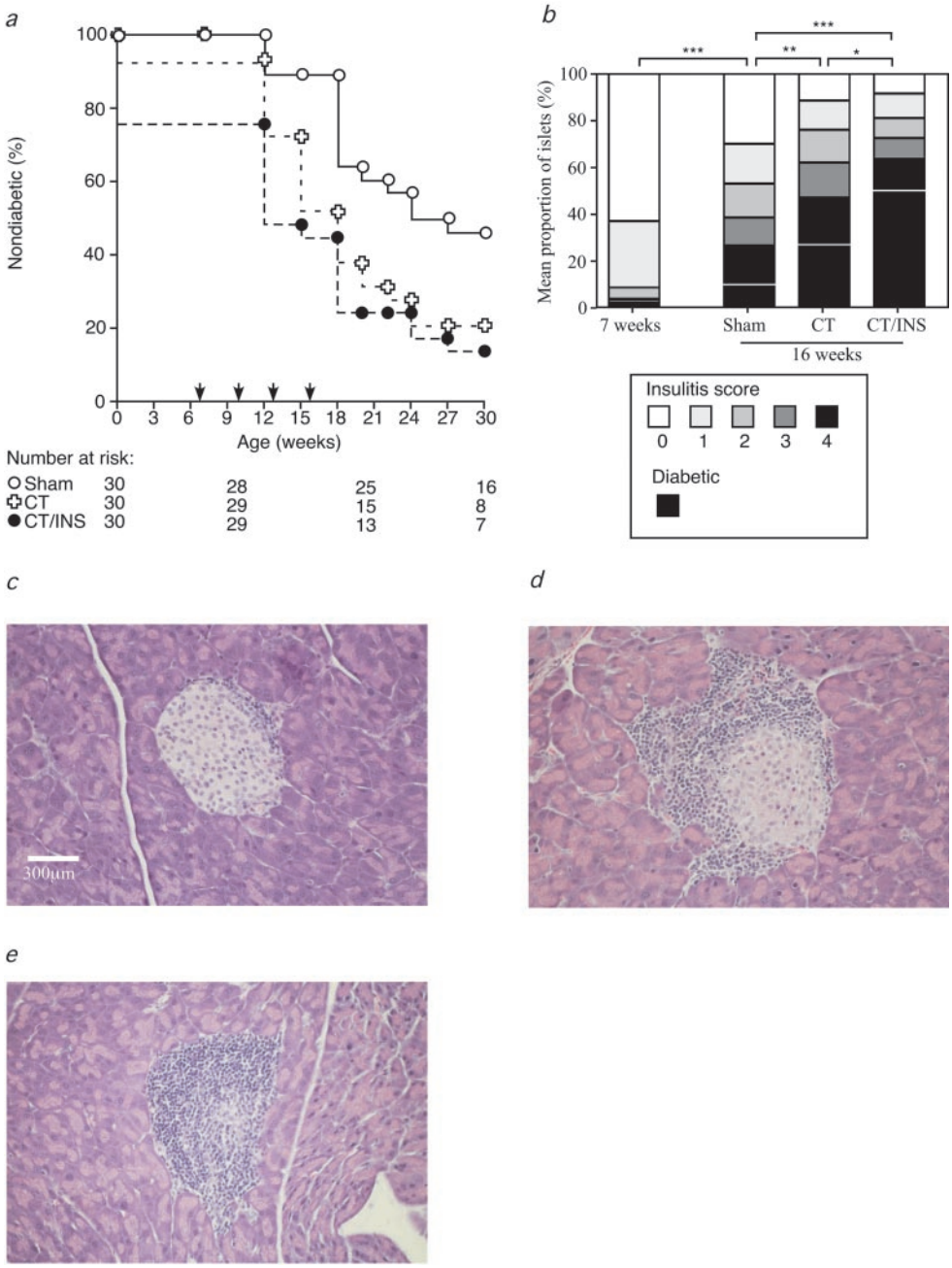

FIGURE 3. Clinical and pathological features of CT/INS B_{9-23}-treated NOD/Lt mice. *a*, Sham (○), CT alone (✣) and CT with INS B_{9-23} (●) immunization (arrows) began at 7 wk of age ($p = 0.002$, log rank test; Hazard ratios, sham = 1.0, CT = 2.2 and CT/INS = 2.8). *b*, Mean insulitis scores for NOD/Lt mice at 7 wk of age ($n = 10$) and following treatment at 16 wk (sham, $n = 8$; CT $n = 5$; and CT/INS B_{9-23}, $n = 6$) (*b*) (*, $p < 0.05$; **, $p < 0.005$; and ***, $p < 0.0001$). Diabetic mice are shown in black. Representative photographs display a typical islet of each treatment group. *c–e*, Islets of mice within the sham-treated group generally displayed relatively low levels of leukocyte infiltration (*c*). Comparatively, mice from CT (*d*) and CT/INS B_{9-23} (*e*)-treated groups displayed increasing degrees of islet inflammation.

of NOD/Lt mice. Pancreatic specimens from diabetic and nondiabetic mice from each group were assigned an insulitis score according to the mean degree of infiltration in individual islets (Fig. 3*b*, see *Materials and Methods*). Consistent with the spontaneous progression of insulitis in NOD/Lt mice, all groups showed significantly greater leukocyte infiltration at 16 weeks of age compared with mice at 7 wk ($p = 0.0001$, Contingency Table Analysis, Fig. 3*b*). However, the CT and CT/INS B_{9-23}-treated mice demonstrated significantly greater degrees of islet infiltration at 16 wk than sham-treated mice of the same age ($p < 0.0001$, Contingency Table Analysis, Fig. 3, *b–e*). Furthermore, there was more islet infiltration in the CT/INS B_{9-23}-treated group compared with CT alone ($p < 0.05$, Contingency Table Analysis, Fig. 3*b*), a trend which matched the clinical status of the mice (vide supra).

Immune response to CT and INS B_{9-23} in NOD/Lt mice

The immunological effects of dermal exposure to CT in NOD/Lt mice mirrored those seen in CT/MOG_{35-55}-treated C57BL/6 mice. Although vigorous IgG anti-CT responses were observed (Fig. 4*a*), anti-INS B_{9-23} peptide Ab responses were muted in CT/INS B_{9-23}-treated mice compared with recipients of CFA/INS B_{9-23} (Fig. 4*b*). Moreover, splenic T cell responses to both CT and peptide, as measured by proliferation, were readily detected (Fig. 4*c*).

To test the effect of dermal CT on inflammation at the level of the target organ, we examined cytokine production by pancreatic islet infiltrating T cells. The proportion of islet T cells secreting IFN-γ, as measured by ELISPOT, was increased in CT-exposed groups compared with sham-treated control mice (Fig. 4*d*) ($p < 0.05$, three-way Kruskal-Wallis test) with the majority of the significance being from the sham vs CT/INS B_{9-23} comparison ($p < 0.02$, Mann-Whitney test). Similarly, the proportion of T cells secreting IL-4 in mice receiving CT with or without INS B_{9-23} was greater than in the sham-treated group (Fig. 4*e*; $p < 0.01$, three-way Kruskal-Wallis test), again with the greatest contribution coming from the sham vs CT/INS B_{9-23} comparison ($p < 0.005$, Mann-Whitney *U* test).

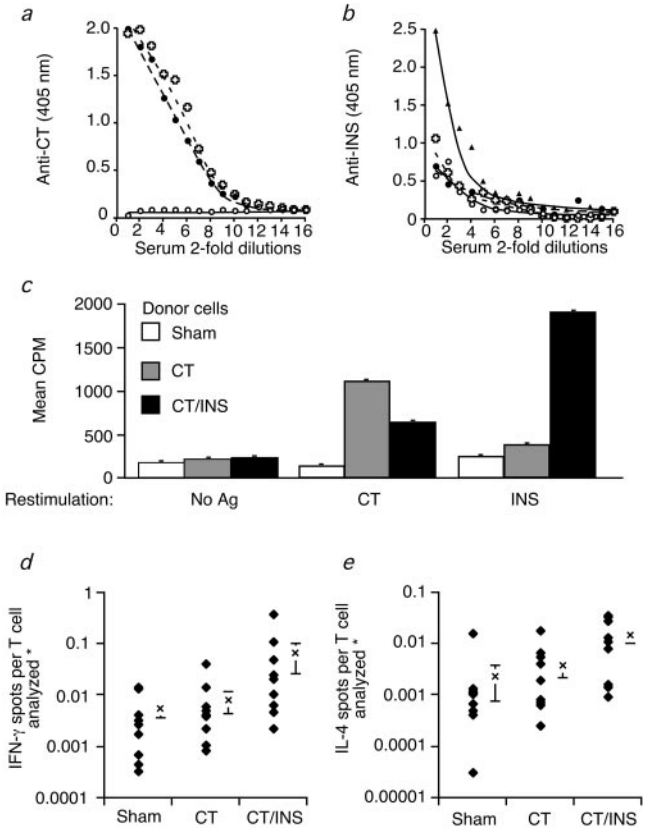

FIGURE 4. Ab and T cell responses to treated NOD/Lt mice. *a* and *b*, Serum collected after three immunization rounds with sham (○), CT (✣), or CT/INS B_{9-23} (●) treatment were analyzed for anti-CT (*a*) and anti-peptide (*b*) IgG-specific Ab responses by ELISA. Anti-peptide Ab response from CFA/INS B_{9-23} immunized mice ($n = 9$, ▲) is shown for comparison. *c*, Mean proliferative responses to CT and INS B_{9-23} of splenic T cells obtained from recipients of sham ($n = 10$), CT ($n = 10$), or CT/INS B_{9-23} ($n = 9$) treatment (mean ± SEM). T cell cytokine responses in the pancreas. *d* and *e*, Islet infiltrating T cell IFN-γ (*d*) (**, $p < 0.02$, and ***, $p < 0.03$) and IL-4 (*e*) (**, $p < 0.02$; ***, $p < 0.02$) production was analyzed by ELISPOT.

Discussion

CT is a potent adjuvant for oral (12), nasal, and transcutaneous (13) immunization. Low amounts of CT can enhance Ag presentation and IL-1 production by APC and dramatically increase T cell priming and proliferation (14–16). There is some suggestion that at least part of this activity can be attributed to direct costimulation of T cells (17).

The data presented in this study suggest that the application of CT to intact skin can induce and enhance the severity of autoimmune pathology. Specifically, dermal exposure to CT, with or without autoantigen, exacerbated the severity of autoimmune disease in two different models. This result is unexpected because, as a generalization, bacterial products with adjuvant activity, including CT, usually decrease the severity of autoimmune tissue destruction in experimental models. For example, systemic administration of *Mycobacterium bovis* (18) or other potent adjuvants such as CFA (18), LPS (19), or CpG oligonucleotide motifs (20, 21) all protect against onset of autoimmune diabetes in NOD mice. Indeed, both oral and intranasal administration of CT conjugated to an appropriate autoantigen enhances self tolerance, thereby inhibiting EAE in Lewis rats (22) and spontaneous type 1 (insulin-dependent) diabetes in NOD mice (23).

The mechanism by which adjuvants modulate autoimmune responses is far from clear. Mucosal administration of CT tends to induce a nonpathogenic Th2 immune response and has been reported to selectively inhibit IL-12 receptor expression and IL-12 secretion (24). Thus, CT B chain conjugated to insulin when given orally to NOD/Lt mice is associated with up-regulation of T cells with a Th2 phenotype (25). In contrast, other groups have reported that CT can enhance both Th1- and Th2-associated cytokines equally. Moreover, the cytokine deviation associated with prevention of autoimmune disease by at least some adjuvants does not appear to be responsible for this effect (26). For example, NOD mice deficient in either IL-4 or IL-10, due to targeted gene deletion, were still protected from type 1 diabetes by either CFA or bacillus Calmette-Guérin (BCG) (27). One possible explanation is that depots of adjuvant at the site of administration become inflammatory foci which disrupt recirculation patterns of activated autoreactive T cells, early in the evolution of the disease process. Consistent with this view is the finding that targeted gene deletion of IFN-γ, a key proinflammatory cytokine, eliminated the diabetes-preventing activity of BCG in NOD mice (27).

Our finding that CT induced (primed for) EAE in C57BL/6 mice when coapplied repeatedly with the autoantigen MOG_{35-55} is con-

sistent with the empiric basis of many models of experimental autoimmunity, namely that the incorporation of an adjuvant such as *Mycobacterium tuberculosis* into oil-in-water emulsions of self Ags dramatically enhances the incidence and severity of induced disease (28). In these cases, as in the current situation where CT/INS B_{9-23} treatment increased the incidence of diabetes in NOD/Lt mice, it is reasonable to assume that repeated, or prolonged (via an Ag/emulsion depot) administration of self Ag together with adjuvant results in activation and expansion of autoreactive T lymphocytes which can recirculate to damage autologous tissues in situ. Presumably, the associated expansion in Ag-specific effectors more than compensates for any interference in recirculation patterns.

More difficult to explain are our findings that the severity of EAE induced by CFA/MOG_{35-55} in C57BL/6 mice, and the incidence and time of onset of diabetes, were both enhanced by repeated dermal application of CT alone. Under these circumstances exposure to CT appears to represent an environmental enhancer of autoimmunity, which by analogy with genetic enhancers, increases the phenotypic expression of an underlying genetic susceptibility to autoimmune disease. T cell proliferative responses to autoantigens were increased and both IFN-γ and IL-4 were secreted in greater amounts by autoantigen-specific splenic T cells in each of the models following dermal application of CT (Fig. 4*c* and data not shown). Therefore, the treatment appears to exert an adjuvant-like effect on autoimmune responses, without inducing the protection from disease normally associated with i.v., s.c., or mucosal administration of bacterial adjuvants. These results suggest that the anatomical site of administration plays an important role in determining response parameters of autoreactive T cells following adjuvant exposure.

We postulate that application of CT to intact skin results in activation of the skin-associated APC, the epidermal Langerhans cells, as such a response is consistent with the known action of CT on other APC (15, 16). Langerhans cells conventionally migrate to the draining lymph node on activation and, at this site, present Ag to responding T cells. Presumably following application of CT alone, T cells specific for CT and/or local self and foreign Ags are generated. These activated T cells may then recirculate to other sites of inflammation, such as those already undergoing autoimmune tissue damage, where they could receive bystander activation signals, contributing to the destructive processes leading to clinical disease. In this situation, unlike those associated with other models of adjuvant activity in autoimmune disease, there would be no local inflammation at the site of administration to recruit activated T cells.

The dermal adjuvant activity of CT is shared with several other bacterial products naturally present in the environment, including the heat labile enterotoxin of *Escherichia coli* (LT), exotoxin A of *Pseudomonas aeruginosa*, a bacterial CpG oligonucleotide motif, and to a lesser extent LPS and muramyl dipeptide (29, 30). This broad range of products is reminiscent of those for which Ag nonspecific responses can be generated via receptors for pathogen-associated molecular patterns, suggesting the possibility that Toll-like receptors (TLR) may mediate the activation of Langerhans cells by these agents. Such a mechanism is consistent with the findings that adoptive transfer of EAE can be facilitated when reactiviation of T cells is performed with APC exposed to CpG oligonucleotides (31) and that the adjuvant activity of CT is affected by allelic differences at the *Lps* locus, which encodes TLR4 (32). If true, the available natural and induced TLR mutant strains could be used for undertaking further analysis of the molecular mechanisms of dermal enhancement.

Together with CT, a number of dermally active adjuvants are being examined in human clinical trials as candidates for a novel transcutaneous vaccination strategy, which has the advantages of low cost and ease of administration (3). Although LT, for instance, has been administered transcutaneously at doses of up to 500 μg to human subjects without significant local toxicity (3), the data presented in this study point to the potential risk of enhanced autoimmunity in genetically susceptible humans following repeated natural or therapeutic contact with intact skin by such bacterial products.

References

1. Glenn, G. M., M. Rao, G. R. Matyas, and C. R. Alving. 1998. Skin immunization made possible by cholera toxin. *Nature 391:851*.
2. Glenn, G. M., T. Scharton-Kersten, R. Vassell, C. P. Mallett, T. L. Hale, and C. R. Alving. 1998. Transcutaneous immunization with cholera toxin protects mice against lethal mucosal toxin challenge. *J. Immunol. 161:3211*.
3. Glenn, G. M., D. N. Taylor, X. Li, S. Frankel, A. Montemarano and C. R. Alving. 2000. Transcutaneous immunization: a human vaccine delivery strategy using a patch. *Nat. Med. 6:1403*.
4. Guerena-Burgueno, F., E. R. Hall, D. N. Taylor, F. J. Cassels, D. A. Scott, M. K. Wolf, Z. J. Roberts, G. V. Nesterova, C. R. Alving, and G. M. Glenn. 2002. Safety and immunogenicity of a prototype enterotoxigenic *Escherichia coli* vaccine administered transcutaneously. *Infect. Immun. 70:1874*.
5. Arrington, J., R. P. Braun, L. Dong, D. H. Fuller, M. D. Macklin, S. W. Umlauf, S. J. Wagner, M. S. Wu, L. G. Payne, and J. R. Haynes. 2002. Plasmid vectors encoding cholera toxin or the heat-labile enterotoxin from *Escherichia coli* are strong adjuvants for DNA vaccines. *J. Virol. 76:4536*.
6. Riminton, D. S., H. Körner, D. H. Strickland, F. A. Lemckert, J. D. Pollard, and J. D. Sedgwick. 1998. Challenging cytokine redundancy: inflammatory cell movement and clinical course of experimental autoimmune encephalomyelitis are normal in lymphotoxin-deficient, but not tumor necrosis factor-deficient, mice. *J. Exp. Med. 187:1517*.
7. Gardinier, M. V., P. Amiguet, C. Linington, and J. M. Matthieu. 1992. Myelin/oligodendrocyte glycoprotein is a unique member of the immunoglobulin superfamily. *J. Neurosci. Res. 33:177*.
8. Daniel, D., and D. R. Wegmann. 1996. Protection of nonobese diabetic mice from diabetes by intranasal or subcutaneous administration of insulin peptide B-(9-23). *Proc. Natl. Acad. Sci. USA 93:956*.
9. Hammond, K. J. L., L. D. Poulton, L. J. Palmisano, P. A. Silveira, D. I. Godfrey, and A. G. Baxter. 1998. α/β-T cell receptor $(TCR)^+CD4^-CD8^-$ (NKT) thymocytes prevent insulin-dependent diabetes mellitus in nonobese diabetic (NOD)/Lt mice by the influence of interleukin (IL)-4 and/or IL-10. *J. Exp. Med. 187:1047*.
10. Tomonari, K. 1998. A rat antibody against a structure functionally related to the mouse T-cell receptor/T3 complex. *Immunogenetics 28:455*.
11. Bernard, C. C., and P. R. Carnegie. 1975. Experimental autoimmune encephalomyelitis in mice: immunologic response to mouse spinal cord and myelin basic proteins. *J. Immunol. 114:1537*.
12. Lycke, N., and J. Holmgren. 1986. Strong adjuvant properties of cholera toxin on gut mucosal immune responses to orally presented antigens. *Immunology 59:301*.
13. Glenn, G., T. Scharton-Kersten, R. Vassell, G. R. Matyas, and C. A. Alving. 1999. Transcutaneous immunization with bacterial ADP-ribosylating exotoxins as antigens and adjuvants. *Infect. Immun. 67:1100*.
14. Lycke, N., A. K. Bromander, L. Ekman, U. Karlsson, and J. Holmgren. 1989. Cellular basis of immunomodulation by cholera toxin in vitro with possible association to the adjuvant function in vivo. *J. Immunol. 142:20*.
15. Bromander, A., J. Holmgren, and N. Lycke. 1991. Cholera toxin stimulates IL-1 production and enhances antigen presentation by macrophages in vitro. *J. Immunol. 146:2908*.
16. Hornquist, E., and N. Lycke. 1993. Cholera toxin adjuvant greatly promotes antigen priming of T cells. *Eur. J. Immunol. 23:2136*.
17. Li, T. K., and B. S. Fox. 1996. Cholera toxin B subunit binding to an antigen-presenting cell directly co-stimulates cytokine production from a T cell clone. *Int. Immunol. 8:1849*.
18. Sadelain, M. W., H. Y. Qin, J. Lauzon, and B. Singh. 1990. Prevention of type I diabetes in NOD mice by adjuvant immunotherapy. *Diabetes 39:583*.
19. Sai, P., and A. S. Rivereau. 1996. Prevention of diabetes in the nonobese diabetic mouse by oral immunological treatments: comparative efficiency of human insulin and two bacterial antigens, lipopolysacharide from *Escherichia coli* and glycoprotein extract from *Klebsiella pneumoniae*. *Diabetes Metab. 22:341*.
20. Quintana, F. J., A. Rotem, P. Carmi, and I. R. Cohen. 2000. Vaccination with empty plasmid DNA or CpG oligonucleotide inhibits diabetes in nonobese diabetic mice: modulation of spontaneous 60-kDa heat shock protein autoimmunity. *J. Immunol. 165:6148*.
21. Coon, B., L. L. An, J. L. Whitton, and M. G. von Herrath. 1999. DNA immunization to prevent autoimmune diabetes. *J. Clin. Invest. 104:189*.
22. Sun, J. B., B. G. Xiao, M. Lindblad, B. L. Li, H. Link, C. Czerkinsky, and J. Holmgren. 2000. Oral administration of cholera toxin B subunit conjugated to myelin basic protein protects against experimental autoimmune encephalomyeli-

tis by inducing transforming growth factor-β-secreting cells and suppressing chemokine expression. *Int. Immunol. 12:1449.*

23. Bergerot, I., C. Ploix, J. Petersen, V. Moulin, C. Rask, N. Fabien, M. Lindblad, A. Mayer, C. Czerkinsky, J. Holmgren, and C. Thivolet. 1997. A cholera toxoid-insulin conjugate as an oral vaccine against spontaneous autoimmune diabetes. *Proc. Natl. Acad. Sci. USA 94:4610.*
24. Braun, M. C., J. He, C. Y. Wu, and B. L. Kelsall. 1999. Cholera toxin suppresses interleukin (IL)-12 production and IL-12 receptor β1 and β2 chain expression. *J. Exp. Med. 189:541.*
25. Ploix, C., I. Bergerot, A. Durand, C. Czerkinsky, J. Holmgren, and C. Thivolet. 1999. Oral administration of cholera toxin B-insulin conjugates protects NOD mice from autoimmune diabetes by inducing $CD4^+$ regulatory T-cells. *Diabetes 48:2150.*
26. Hornquist, E., and N. Lycke. 1995. Cholera toxin increases T lymphocyte responses to unrelated antigens. *Adv. Exp. Med. Biol. 371B:1507.*
27. Serreze, D. V., H. D. Chapman, C. M. Post, E. A. Johnson, W. L. Suarez-Pinzon, and A. Rabinovitch. 2001. Th1 to Th2 cytokine shifts in nonobese diabetic mice: sometimes an outcome, rather than the cause, of diabetes resistance elicited by immunostimulation. *J. Immunol. 166:1352.*
28. Freund, J., E. R. Stern, and T. M. Pisani. 1947. Isoallergic encephalomyelitis and radiculitis in guinea pigs after one injection of brain and mycobacteria in water-in-oil emulsion. *J. Immunol. 57:179.*
29. Scharton-Kersten, T. J. Yu, R. Vassell, D. O'Hagan, C. R. Alving, and G. M. Glenn. 2000. Transcutaneous immunization with bacterial ADP-ribosylating exotoxins, subunits, and unrelated adjuvants. *Infect. Immun. 68:306.*
30. Freytag, L. C., and J. D. Clements. 1999. Bacterial toxins as mucosal adjuvants. *Curr. Top. Microbiol. Immunol. 236:215.*
31. Ichikawa, H. T., L. P. Williams, and B. M. Segal. 2002. Activation of APCs through CD40 or Toll-like receptor 9 overcomes tolerance and precipitates autoimmune disease. *J. Immunol. 169:2781.*
32. Elson, C. O. 1992. Cholera toxin as a mucosal adjuvant: effects of H-2 major histocompatibility complex and *lps* genes. *Infect. Immun. 60:2874.*